

# Probing microscopic conformational dynamics in folding reactions by measuring transition paths

Noel Q. Hoffer, Michael T. Woodside

*Department of Physics, University of Alberta, Edmonton AB, T6G 2E1, Canada*

**Abstract:** Transition paths comprise those parts of a folding trajectory where the molecule passes through the high-energy transition states separating folded and unfolded conformations. The transition states determine the folding kinetics and mechanism but are difficult to observe because of their brief duration. Single-molecule experiments have in recent years begun to characterize transition paths in folding reactions, allowing the microscopic conformational dynamics that occur as a molecule traverses the energy barriers to be probed directly. Here we review single-molecule fluorescence and force spectroscopy measurements of transition-path properties, including the time taken to traverse the paths, the local velocity along them, the path shapes, and the variability within these measurements reflecting differences between individual barrier crossings. We discuss how these measurements have been related to theories of folding as diffusion over an energy landscape to deduce properties such as the diffusion coefficient, and how they are being combined with simulations to obtain enhanced atomistic understanding of folding. The richly detailed information available from transition path measurements holds great promise for improved understanding of microscopic mechanisms in folding.

## Introduction

Understanding how proteins and nucleic acids fold into complex structures has been an important goal for decades. Decades of work has established a comprehensive theoretical framework for describing folding as a diffusive search over a multi-dimensional conformational energy landscape [1]. In this picture, the most important parts of the reaction involve passage through the high-energy transition states forming barriers between stable or metastable states, since these states dominate the reaction kinetics, and the paths through these states—known as transition paths (TPs) (Fig. 1)—encapsulate all the critical mechanistic information. Because transition paths (TPs) have a very brief duration, whereas most of the time spent during folding reactions involves non-productive fluctuations that do not cross the energy barrier, they have proven challenging to study experimentally [2]. Furthermore, because TPs are stochastic but the folding of ensembles of molecules cannot be synchronized, single-molecule approaches are needed to observe them. As a result, study of TPs was until recently restricted to theory and simulation [3–9].

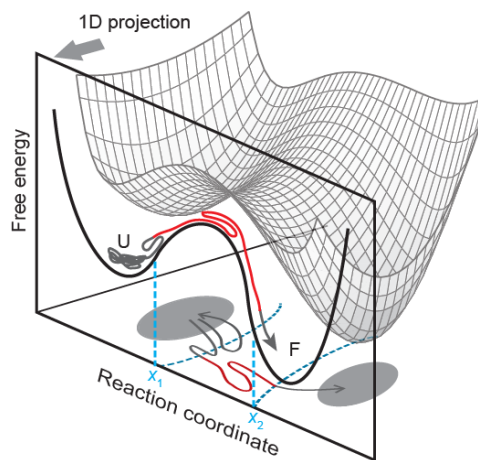


**Fig. 1: Transition paths.** Transition paths represent productive fluctuations (red) that cross the barrier between unfolded (U) and folded (F) states, and ignore non-productive fluctuations (grey). Motions over the multi-dimensional landscape are usually projected onto a 1D reaction coordinate. Adapted from [20\*\*] with permission.

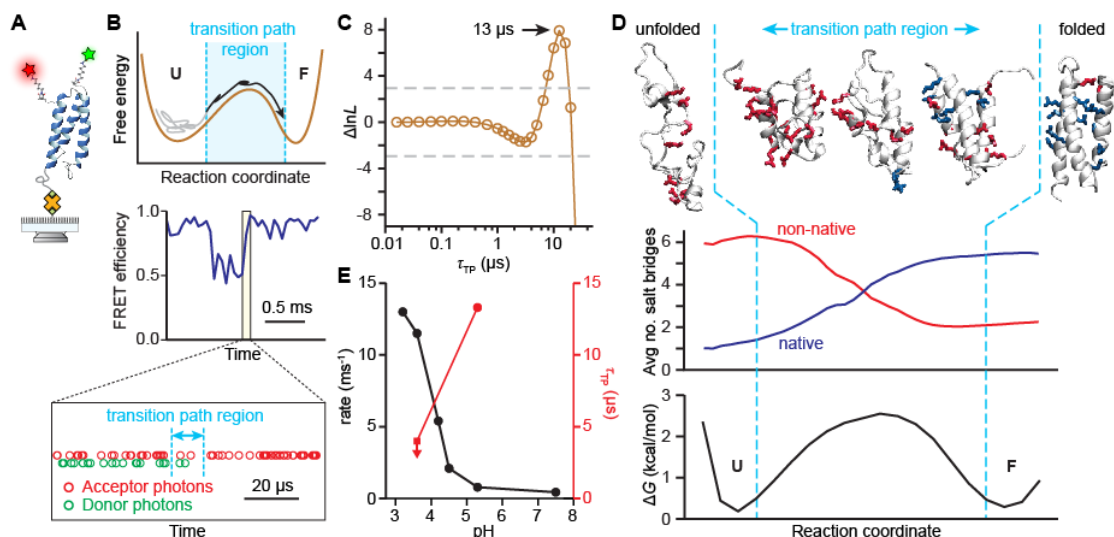


**Figure 2: smFRET measurements of transition-path times.** (A) Schematic of measurement showing FRET dye pair attached to the protein  $\alpha_3D$ . (B) To measure the average time to cross the barrier region (top, cyan), FRET trajectories (middle, blue) typically have insufficient resolution because the minimum averaging window is too large, but analyzing photon arrival statistics (bottom) can identify the most likely  $\tau_{TP}$ . (C) Maximum-likelihood analysis of photon statistics for  $\alpha_3D$  yields  $\tau_{TP} \sim 13 \mu s$ . (D) All-atom simulations of  $\alpha_3D$  folding show non-native salt bridges play a key role in generating internal friction slowing  $\tau_{TP}$ ; the total number of salt bridges remains close to constant as native bridges (blue) replace non-native ones (red) along the transition paths. (E) The transition path time decreases when salt bridges are disfavored by lowering pH, in roughly the same proportion as the folding rate increases, indicating the changes arise from reducing the internal friction. Figures adapted from [13], [14], and [20\*\*] with permission.

In recent years, however, advances in single-molecule instrumentation and analysis have allowed direct measurement of TPs, opening up a new window on the microscopic conformational dynamics during folding. Two methods have been used to characterize TPs experimentally: single-molecule Förster resonance energy transfer (smFRET), wherein resonant energy transfer reports on inter-dye distance changes caused by unfolding/refolding [10]; and single-molecule force spectroscopy (SMFS), wherein length changes in response to tension applied by a force probe like optical tweezers are used to monitor unfolding/refolding [11]. Here we review recent single-molecule studies of TP properties such as the average TP time, TP time distribution, local velocity, and average path shape, examining how comparisons to theory and simulation have yielded new insights into the microscopic features of folding.

### smFRET measurements of average transition-path times in folding

The first direct measurements of TPs were done in pioneering work by Eaton and colleagues using smFRET (Fig. 2A) to determine the average transition-path time,  $\tau_{TP}$ . Traditional FRET analysis has insufficient time resolution to detect individual TPs, because of the binning of time-points needed to calculate FRET values, but by applying a maximum-likelihood analysis of photon-by-photon trajectories [12],  $\tau_{TP}$  could be deduced as the lifetime of a virtual intermediate state (Fig. 2B). It was measured for two small proteins, a fast-folding  $\beta$ -structured WW domain [13] and the engineered helical protein  $\alpha_3D$  [14], and an upper bound was placed on  $\tau_{TP}$  for the  $\alpha\beta$ -structured protein GB1 [13] and a DNA hairpin [15]. For the WW domain,  $\tau_{TP}$  was estimated as  $\sim 2 \mu s$  in standard aqueous solvent, very close to the result obtained in atomistic simulations [16] and not far from the putative protein folding ‘speed limit’ of  $\sim 0.1$ – $1 \mu s$  for small proteins

[17], whereas for  $\alpha_3D$ ,  $\tau_{TP} \sim 13 \mu s$  (Fig. 2C); the upper bound for GB1 was  $10 \mu s$ , and that for the hairpin was  $2.5 \mu s$ .

Crucially, these results clustered closely in the range  $\sim 1\text{--}10 \mu s$ . In contrast, the folding rates of these molecules varied by as much as four orders of magnitude. The fact that  $\tau_{TP}$  varies much less than the folding time,  $\tau_f$  (the inverse of the folding rate), reflects a key property of TPs: since by definition a molecule on a TP always receives sufficient thermal energy to cross the barrier,  $\tau_{TP}$  is relatively insensitive to barrier height, as opposed to  $\tau_f$ , which is dominated by the time a molecule must wait for energy fluctuations large enough to allow barrier crossing. These concepts are captured theoretically by Kramers' expression for  $\tau_f$  [18] and Szabo's expression for  $\tau_{TP}$  [19] in the harmonic-barrier approximation:

$$\tau_f = \frac{2\pi k_B T}{D \sqrt{\kappa_w \kappa_b}} \exp(\Delta G^\ddagger / k_B T) \text{ and } \tau_{TP} = \frac{k_B T \ln(2e^\gamma \Delta G^\ddagger / k_B T)}{D \kappa_b}, \quad (1)$$

where  $k_B T$  is the thermal energy,  $\Delta G^\ddagger$  the barrier height,  $\kappa_{b/w}$  the stiffness of the energy barrier/well, and  $D$  the diffusion coefficient—the fundamental descriptor relating transition kinetics to landscape thermodynamics. Because  $\tau_f$  is exponentially more sensitive to  $\Delta G^\ddagger$  than  $D$ ,  $D$  is very difficult to quantify reliably from rates, as any changes in  $\Delta G^\ddagger$  overwhelm effects from  $D$ . In contrast,  $\tau_{TP}$  varies little with  $\Delta G^\ddagger$ , making it relatively much more sensitive to  $D$ .

This sensitivity of  $\tau_{TP}$  to  $D$  was exploited by Chung & Eaton to show that the large  $\tau_{TP}$  of  $\alpha_3D$  arises from substantial internal friction, reflecting roughness in the energy landscape [14]. By comparing  $\tau_{TP}$  measurements directly to all-atom molecular dynamics simulations of the TPs, the mechanism underlying the internal friction was deduced and found to involve formation of non-native salt bridges [20\*\*] (Fig. 2D). This mechanism was confirmed by showing that at low pH, where the salt bridges were disrupted by protonation,  $\tau_f$  and  $\tau_{TP}$  both decreased in roughly the same proportion, reflecting an increase in  $D$  from removal of the salt bridges (Fig. 2E). Intriguingly,  $\alpha_3D$  is thus an exception to the general expectation that non-native interactions do not play key roles in folding mechanisms [21], suggesting that folding of engineered proteins may differ from that of naturally evolved molecules by having rougher landscapes [22] leading to slower diffusion. Combining measurements and atomistic simulations of TPs as done here, where the timescales of both experiment and simulation overlap directly, provides an exciting and uniquely powerful approach for gaining mechanistic insight into the microscopic dynamics of folding.

### Force spectroscopy measurements of individual transition paths

An alternate approach to measuring TPs using SMFS (Fig. 3A) was developed by Woodside and colleagues. In contrast to fluorescence measurements, where FRET trajectories typically have insufficient resolution to discern individual TPs, SMFS measurements using optical tweezers can obtain resolution of  $\sim 5\text{--}10 \mu s$ , allowing direct observation of individual TPs in molecules with relatively slow diffusion. Thousands of transitions can be measured from a single molecule, allowing robust statistical characterization of the ensemble of TPs. SMFS was used to observe TPs in both nucleic acid hairpin folding [23\*\*,24\*] (Fig. 3B) and prion protein misfolding [23\*\*,25]. These measurements revealed a very broad distribution of TP times,  $p(t_{TP})$ , reflecting statistically independent and highly variable but time-reversal symmetric behavior in each transition as the barrier was crossed diffusively (Fig. 3C). Values for  $\tau_{TP}$  matched those predicted via Eq. 1 from energy landscape reconstructions [26,27], and approximating the

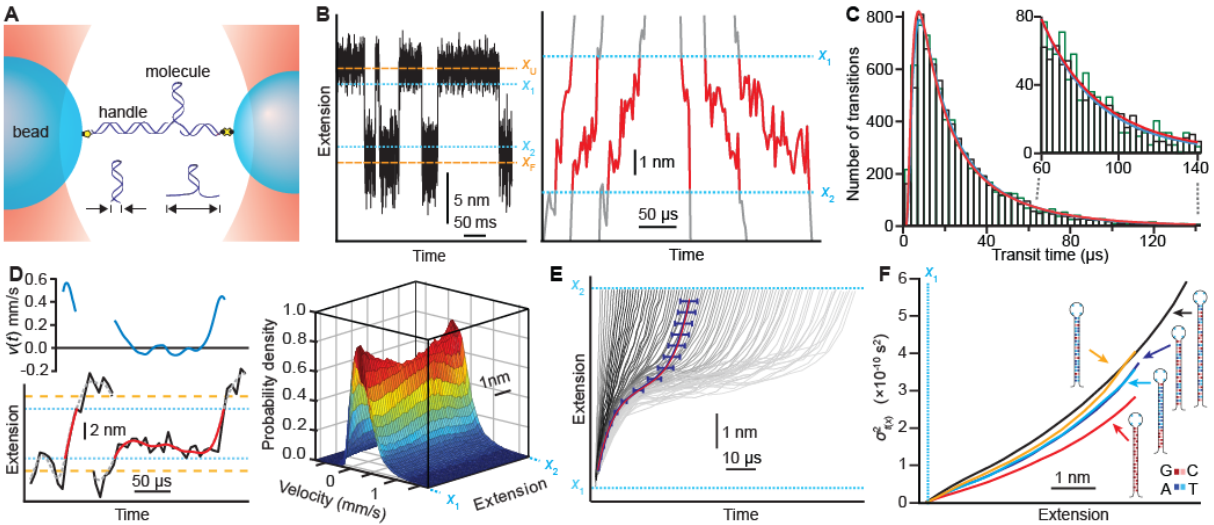


**Figure 3: SMFS measurements of individual transition paths.** (A) Schematic of measurement showing molecule of interest tethered via handles to beads held in optical traps; the folding reaction is monitored through changes in the molecular length. (B) Extension trajectory of a DNA hairpin (black), showing individual unfolding and refolding TPs (red). (C) The distributions of unfolding (black) and refolding (green) TP times from a single hairpin molecule are well fit (red: unfolding, blue: refolding) to the theory for harmonic barriers. (D) TP velocities calculated from smoothed trajectories (right: red) show distinct local variations (right: blue), with a Gaussian-like distribution everywhere along the TPs (left). (E) The average TP shape calculated by averaging all paths of a given duration in the time domain (grey) and then averaging the results in the extension domain (blue) shows a distinctive curvature and is well fit by the path of least effective action for a harmonic barrier (red). (F) The variance in TP shapes as a function of reaction coordinate shows sequence-dependent differences, indicating a sequence-dependent diversity of the TPs being sampled. Figures adapted from [23\*\*], [31\*], and [37\*].

exponential decay of  $p(t_{TP})$  in the Kramers limit [6,28] yielded estimates of  $D$  that agreed well with the results obtained from analyzing rates [25\*,29]. Interestingly,  $\tau_{TP}$  was orders of magnitude larger for prion protein misfolding—500  $\mu\text{s}$ —than for native folding—2  $\mu\text{s}$ , as estimated from Eq. 1 [30]—implying that misfolding landscapes are much rougher, possibly because evolution selects for efficient native folding but not misfolding.

SMFS measurements also revealed high local variability in TPs: transitions could be slow within some parts of the barrier but fast within others. The distribution of local velocities within TPs in DNA hairpin folding [31\*] was close to Gaussian along the whole transition, as expected for a harmonic barrier [32], with a significant tail at negative velocities reflecting the ubiquitous reversals characteristic of diffusive motion (Fig. 3D). This work also highlighted the fundamentally diffusive nature of folding by quantifying the suppression of folding rates by barrier re-crossing as encapsulated in the transmission factor,  $\kappa$ , from classic transition-state theory [18], something that had not previously been done for folding reactions. Calculating  $\kappa$  from TP velocities, barrier re-crossing was found to suppress the rates by  $10^5$ – $10^6$ -fold from the expectation of transition-state theory, which assumes no re-crossing.

Although most TP work to date has focused on transitions in equilibrium folding trajectories, non-equilibrium TPs may provide additional insight by exploring parts of the landscape rarely visited in equilibrium. Gladrow *et al.* made the first measurements of TPs out of equilibrium, studying DNA hairpins [33]. They found a distinct asymmetry in  $p(t_{TP})$  between unfolding and

refolding, with the latter displaying a systematic shift toward shorter times. This asymmetry was attributed to intermediate states induced by the non-equilibrium conditions.

Recent work has also begun to go beyond distributions of TP properties and examine the information about the temporal sequence of events within TPs, as encoded in transition-path shapes. The properties of average TP shapes were explored theoretically [32,34–36] before being measured in nucleic acid hairpins [37\*\*]. The average shapes were observed to be well-described by the path of least effective action for a harmonic barrier (Fig. 3E), returning a diffusion coefficient consistent with estimates from other TP properties. Most interestingly, the variance in path shape around the average showed systematic differences between different hairpins (Fig. 3F), indicating sequence-dependent diversity within the TPs sampled in different molecules. This work opens the possibility of using transition-path shapes to observe directly the statistical multiplicity of routes taken through the energy landscape during folding, including rarely populated routes through unusual pathways and barriers.

### Comparison of experiment and theory

From their inception, TP measurements have been closely coupled with theory to characterize fundamental features of folding quantitatively. The results have been remarkably consistent with expectations for landscape theory, from the excellent self-consistency of diffusion coefficients extracted from numerous different quantities ( $\tau_{\text{TP}}$ ,  $p(t_{\text{TP}})$ , TP velocities, TP shapes [31\*]) to the statistics of the TP occupancy [38,39]. Several theoretical predictions have been validated through TP measurements, including an identity relating  $\tau_{\text{TP}}$  and rates [4], which was found to hold over a wide range of rates [23\*\*,40], and identities relating TP occupancy and velocity profiles [32,41] as well as velocity and committor functions [40]. Other work has extended approximations for TP properties to the small-barrier limit relevant in many experiments [41,42], for improved analysis, and shown that both the logarithmic dependence of  $\tau_{\text{TP}}$  on  $\Delta G^\ddagger$  and the exponential decay of  $p(t_{\text{TP}})$  are general features even under non-idealized conditions including memory effects and non-thermal noise [43].

Most intriguing, in some ways, are the features that do not match expectations of simple theories. One particularly interesting disagreement is that the energy barriers implied by fitting  $p(t_{\text{TP}})$  to theory are very small [23\*\*], much smaller than the barriers found from kinetic and thermodynamic analyses [26,44]. This discrepancy has been attributed to various effects, including the role of entropy in the barrier [45], the dependence of TPs on a different type of barrier than rates [46], anomalous diffusion at short time scales [47], and memory effects in the dynamics [48] and/or non-thermal noise [43]. Another interesting discrepancy with theory is that the average velocity profile showed a local maximum near the barrier top [31\*], instead of a minimum as expected for a harmonic barrier with constant diffusion [32]. This difference may reflect spatial variation in the diffusion coefficient, which is expected to arise from projecting molecular motions in the full multi-dimensional phase space onto a 1D reaction coordinate [49] but has proven difficult to quantify reliably from other measurements [50].

### Transition paths in protein-protein complexes

Although most TP measurements have focused on unimolecular folding reactions, recent work has extended the methods described above to study coupled binding and folding—where two molecules bind and then reconfigure to form the final folded structure—and characterize the resulting encounter complex. Sturzenegger *et al.* [51\*\*] used smFRET to examine the association of two intrinsically disordered proteins, ACTR and NCBD, which form stable folded

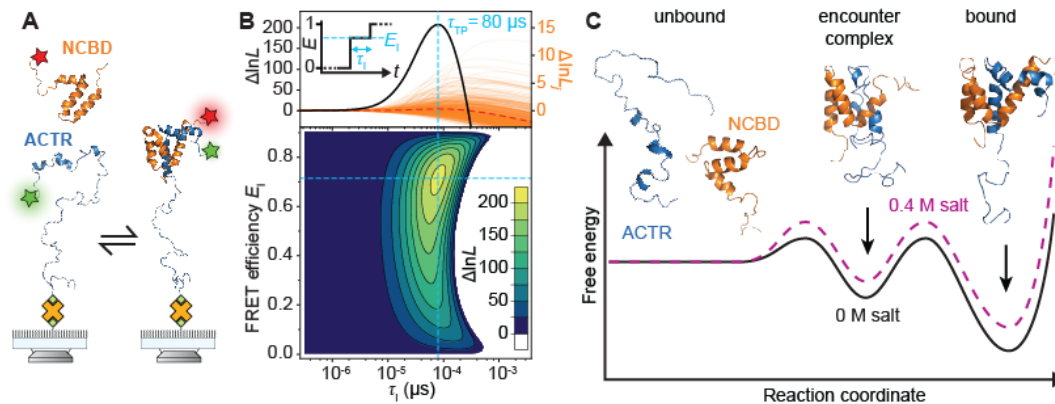


**Figure 4: Measuring TPs in an encounter complex.** (A) Measurement schematic showing FRET dye labels attached to two disordered proteins that bind and then fold. (B) Analysis of photon arrival statistics treating TP as a virtual intermediate (top, inset) reveals most likely TP times for each transition (top, orange), overall average  $\tau_{TP} = 80 \mu\text{s}$  (top, black), and distribution of TP time and FRET value likelihoods (bottom). (C) The long TP times arises from a high-energy intermediate with salt-dependent barriers rather than high internal friction. Figures adapted from [51\*\*] according to Creative Commons licence <http://creativecommons.org/licenses/by/4.0/>

dimers upon binding (Fig. 4A), applying maximum-likelihood analysis to discern a transition intermediate wherein the proteins were bound but not yet folded. They found that this complex was much longer-lived than the transition paths observed in unimolecular folding, with  $\tau_{TP} \sim 80 \mu\text{s}$ , allowing the most likely duration of individual TPs to be estimated from the FRET signal (Fig 4B). Ruling out internal friction effects as the origin of the large  $\tau_{TP}$ ,  $p(t_{TP})$  was found to be most consistent with local barriers around a high-energy intermediate (Fig. 4C), where encounter-complex formation was driven electrostatically but subsequent folding dominated by hydrophobic effects. Kim *et al.* [52\*\*] used a similar approach to compare the encounter-complex lifetime for the disordered proteins NCBD and TAD to that of the ordered proteins barnase and barstar. The TAD/NCBD encounter-complex lifetime, in the range 180–630  $\mu\text{s}$ , was found to be at least two orders of magnitude longer than that of barnase/barstar (2–12  $\mu\text{s}$ ). The salt dependence of the  $\tau_{TP}$  values suggested that the TAD/NCBD encounter complex is stabilized by non-native electrostatic interactions, allowing rapid dimer formation before slower reorganization into the native fold; such non-native interactions are lacking in the barnase/barstar complex because both proteins are already natively folded, leading to shorter complex lifetimes. These studies highlight the potential to extend TP measurements to illuminate the microscopic dynamics of the many multi-protein complexes that play essential roles in biological processes.

## Outlook

Experimental studies of TPs are relatively young, with much of the vast information they contain about folding mechanisms still to be explored, technical capabilities still developing, and most studies prompting new questions to be answered. Theories that will complement future experiments continue to be developed, for example providing frameworks for describing different shapes of barriers [53], exploring inertial effects in TPs [54,55], improving methods for simulating TPs [56], and developing methods for predicting TPs and their statistics [57,58]. The effects of experimental design on TP measurements are being explored to identify conditions for reliable measurements [36,59–61]. Advances in instrumentation continue to push forward experimental frontiers, such as improved AFM cantilevers enabling  $\mu\text{s}$ -resolution measurements

of both globular [62] and membrane proteins [63\*]. There is also much room for further integration of atomistic simulations with TP measurements, as well as comparisons of TP measurements to ultrafast kinetic measurements of downhill folding [64]. These advances provide exciting opportunities for increasingly detailed characterization of the microscopic dynamics in folding reactions, not only for model systems that can elucidate the fundamental biophysics of folding, but also more complex systems where TP dynamics may inform on biological function.

**Acknowledgements:** This work was supported by the Natural Sciences and Engineering Research Council of Canada and the John Simon Guggenheim Foundation.

## References

1. Onuchic JN, Wolynes PG: Theory of protein folding. *Curr Opin Struct Biol* 2004, **14**:70–75.
2. Chung HS: Transition Path Times Measured by Single-Molecule Spectroscopy. *J Mol Biol* 2018, **430**:409–423.
3. Bolhuis PG, Chandler D, Dellago C, Geissler PL: TRANSITION PATH SAMPLING: Throwing Ropes Over Rough Mountain Passes, in the Dark. *Annu Rev Phys Chem* 2002, **53**:291–318.
4. Hummer G: From transition paths to transition states and rate coefficients. *J Chem Phys* 2004, **120**:516–523.
5. Best RB, Hummer G: Reaction coordinates and rates from transition paths. *Proc Natl Acad Sci USA* 2005, **102**:6732–6737.
6. Zhang BW, Jasnow D, Zuckerman DM: Transition-event durations in one-dimensional activated processes. *J Chem Phys* 2007, **126**:074504.
7. Sega M, Faccioli P, Pederiva F, Garberoglio G, Orland H: Quantitative Protein Dynamics from Dominant Folding Pathways. *Phys Rev Lett* 2007, **99**:118102.
8. Jayachandran G, Vishal V, Pande VS: Using massively parallel simulation and Markovian models to study protein folding: Examining the dynamics of the villin headpiece. *J Chem Phys* 2006, **124**:164902.
9. Piana S, Lindorff-Larsen K, Shaw DE: Protein folding kinetics and thermodynamics from atomistic simulation. *Proc Natl Acad Sci USA* 2012, **109**:17845–17850.
10. Ha T: Single-Molecule Fluorescence Resonance Energy Transfer. *Methods* 2001, **25**:78–86.
11. Ritchie DB, Woodside MT: Probing the structural dynamics of proteins and nucleic acids with optical tweezers. *Curr Opin Struct Biol* 2015, **34**:43–51.
12. Gopich IV, Szabo A: Decoding the Pattern of Photon Colors in Single-Molecule FRET. *J Phys Chem B* 2009, **113**:10965–10973.

13. Chung HS, McHale K, Louis JM, Eaton WA: Single-Molecule Fluorescence Experiments Determine Protein Folding Transition Path Times. *Science* 2012, **335**:981–984.
14. Chung HS, Eaton WA: Single-molecule fluorescence probes dynamics of barrier crossing. *Nature* 2013, **502**:685–688.
15. Truex K, Sung Chung H, Louis JM, Eaton WA: Testing Landscape Theory for Biomolecular Processes with Single Molecule Fluorescence Spectroscopy. *Phys Rev Lett* 2015, **115**:018101.
16. Lindorff-Larsen K, Piana S, Dror RO, Shaw DE: How fast-folding proteins fold. *Science* 2011, **334**:517–520.
17. Kubelka J, Hofrichter J, Eaton WA: The protein folding ‘speed limit.’ *Curr Opin Struct Biol* 2004, **14**:76–88.
18. Hänggi P, Talkner P, Borkovec M: Reaction-rate theory: fifty years after Kramers. *Rev Mod Phys* 1990, **62**:251–341.
19. Chung HS, Louis JM, Eaton WA: Experimental determination of upper bound for transition path times in protein folding from single-molecule photon-by-photon trajectories. *Proc Natl Acad Sci USA* 2009, **106**:11837–11844.
- 20\*\*. Chung HS, Piana-Agostinetti S, Shaw DE, Eaton WA: Structural origin of slow diffusion in protein folding. *Science* 2015, **349**:1504–1510.  
 Combines experimental measures of transition-path times with all-atom molecular dynamics simulations to pinpoint non-native salt bridge formation as the mechanism for slow diffusion in the folding of the engineered protein  $\alpha_3D$ .
21. Best RB, Hummer G, Eaton WA: Native contacts determine protein folding mechanisms in atomistic simulations. *Proc Natl Acad Sci USA* 2013, **110**:17874–17879.
22. Basak S, Nobrega RP, Tavella D, Deveau LM, Koga N, Tatsumi-Koga R, Baker D, Massi F, Matthews CR: Networks of electrostatic and hydrophobic interactions modulate the complex folding free energy surface of a designed  $\beta\alpha$  protein. *Proc Natl Acad Sci USA* 2019, **116**:6806–6811.
- 23\*\*. Neupane K, Foster DAN, Dee DR, Yu H, Wang F, Woodside MT: Direct observation of transition paths during the folding of proteins and nucleic acids. *Science* 2016, **352**:239–242.  
 Provides the first direct visualization of transition path trajectories in folding reactions and measures the distribution of transition-path times for a DNA hairpin and a misfolded protein, revealing features of the folding such as the diffusion coefficient (much slower for protein misfolding than native folding) and the apparent barrier for transition paths (smaller than expected from the rates).

- 24\*. Neupane K, Wang F, Woodside MT: Direct measurement of sequence-dependent transition path times and conformational diffusion in DNA duplex formation. *Proc Natl Acad Sci USA* 2017, **114**: 1329-1334.
- Using transition-path time measurements to calculate the conformational diffusion coefficient for DNA hairpins of different sequences, finds that folding of G:C base-pairs involves faster diffusion than A:T pairs.
25. Yu H, Dee DR, Liu X, Brigley AM, Sosova I, Woodside MT: Protein misfolding occurs by slow diffusion across multiple barriers in a rough energy landscape. *Proc Natl Acad Sci USA* 2015, **112**:8308–8313.
26. Woodside MT, Anthony PC, Behnke-Parks WM, Larizadeh K, Herschlag D, Block SM: Direct Measurement of the Full, Sequence-Dependent Folding Landscape of a Nucleic Acid. *Science* 2006, **314**:1001–1004.
27. Woodside MT, Block SM: Reconstructing Folding Energy Landscapes by Single-Molecule Force Spectroscopy. *Annu Rev Biophys* 2014, **43**:19–39.
28. Chaudhury S, Makarov DE: A harmonic transition state approximation for the duration of reactive events in complex molecular rearrangements. *J Chem Phys* 2010, **133**:034118.
29. Neupane K, Ritchie DB, Yu H, Foster DAN, Wang F, Woodside MT: Transition Path Times for Nucleic Acid Folding Determined from Energy-Landscape Analysis of Single-Molecule Trajectories. *Phys Rev Lett* 2012, **109**:068102.
30. Yu H, Gupta AN, Liu X, Neupane K, Brigley AM, Sosova I, Woodside MT: Energy landscape analysis of native folding of the prion protein yields the diffusion constant, transition path time, and rates. *Proc Natl Acad Sci USA* 2012, **109**:14452–14457.
- 31\*. Neupane K, Hoffer NQ, Woodside MT: Measuring the Local Velocity along Transition Paths during the Folding of Single Biological Molecules. *Phys Rev Lett* 2018, **121**:018102.
- Presents the first measurements of TP velocities along the reaction coordinate and calculates the transmission factor that quantifies the degree to diffusive barrier re-crossing suppresses folding rates compared to classic transition-state theory.
32. Makarov DE: Shapes of dominant transition paths from single-molecule force spectroscopy. *J Chem Phys* 2015, **143**:194103.
33. Gladrow J, Ribezzi-Crivellari M, Ritort F, Keyser UF: Experimental evidence of symmetry breaking of transition-path times. *Nat Commun* 2019, **10**:55.
34. Faccioli P, Sega M, Pederiva F, Orland H: Dominant Pathways in Protein Folding. *Phys Rev Lett* 2006, **97**:108101.
35. Kim WK, Netz RR: The mean shape of transition and first-passage paths. *J Chem Phys* 2015, **143**:224108.

36. Cossio P, Hummer G, Szabo A: Transition paths in single-molecule force spectroscopy. *J Chem Phys* 2018, **148**:123309.
- 37\*\*. Hoffer NQ, Neupane K, Pyo AGT, Woodside MT: Measuring the average shape of transition paths during the folding of a single biological molecule. *Proc Natl Acad Sci USA* 2019, **116**: 8125-8130.  

Describes how to measure average shapes of TPs, showing that for DNA hairpins they fit well to one-dimensional diffusion over a harmonic barrier and finding a sequence-dependent differences in the diversity of TPs that are populated.
38. Neupane K, Manuel AP, Lambert J, Woodside MT: Transition-Path Probability as a Test of Reaction-Coordinate Quality Reveals DNA Hairpin Folding Is a One-Dimensional Diffusive Process. *J Phys Chem Lett* 2015, **6**:1005–1010.
39. Neupane K, Manuel AP, Woodside MT: Protein folding trajectories can be described quantitatively by one-dimensional diffusion over measured energy landscapes. *Nat Phys* 2016, **12**:700–703.
40. Neupane K, Hoffer NQ, Woodside MT: Testing Kinetic Identities Involving Transition-Path Properties Using Single-Molecule Folding Trajectories. *J Phys Chem B* 2018, doi:10.1021/acs.jpcc.8b05355.
41. Berezhkovskii AM, Makarov DE: Communication: Transition-path velocity as an experimental measure of barrier crossing dynamics. *J Chem Phys* 2018, **148**:201102.
42. Pyo AGT, Hoffer NQ, Neupane K, Woodside MT: Transition-path properties for folding reactions in the limit of small barriers. *J Chem Phys* 2018, **149**:115101.
43. Carlon E, Orland H, Sakaue T, Vanderzande C: Effect of Memory and Active Forces on Transition Path Time Distributions. *J Phys Chem B* 2018, **122**:11186–11194.
44. Dudko OK, Hummer G, Szabo A: Theory, analysis, and interpretation of single-molecule force spectroscopy experiments. *Proc Natl Acad Sci USA* 2008, **105**:15755–15760.
45. Makarov DE: Reconciling transition path time and rate measurements in reactions with large entropic barriers. *J Chem Phys* 2017, **146**:071101.
46. Pollak E: Transition Path Time Distribution, Tunneling Times, Friction, and Uncertainty. *Phys Rev Lett* 2017, **118**:070401.
47. Satija R, Das A, Makarov DE: Transition path times reveal memory effects and anomalous diffusion in the dynamics of protein folding. *J Chem Phys* 2017, **147**:152707.
48. Medina E, Satija R, Makarov DE: Transition Path Times in Non-Markovian Activated Rate Processes. *J Phys Chem B* 2018, **122**:11400–11413.
49. Best RB, Hummer G: Coordinate-dependent diffusion in protein folding. *Proc Natl Acad Sci USA* 2010, **107**:1088–1093.

50. Foster DAN, Petrosyan R, Pyo AGT, Hoffmann A, Wang F, Woodside MT: Probing Position-Dependent Diffusion in Folding Reactions Using Single-Molecule Force Spectroscopy. *Biophys J* 2018, **114**:1657–1666.
- 51\*\*. Sturzenegger F, Zosel F, Holmstrom ED, Buholzer KJ, Makarov DE, Nettels D, Schuler B: Transition path times of coupled folding and binding reveal the formation of an encounter complex. *Nat Commun* 2018, **9**:4708.
- Applies maximum-likelihood analysis of smFRET data to measure the coupled binding and folding of two intrinsically disordered proteins, finding a transient intermediate encounter complex where the proteins are bound but not yet folded.
- 52\*\*. Kim J, Meng F, Yoo J, Chung HS. Diffusion-limited association of disordered protein by non-native electrostatic interactions. *Nat Commun* 2018, **9**: 4707
- Uses photon-by-photon analysis to compare the lifetimes of transient encounter complexes for proteins which require binding prior to folding and proteins which are folded prior to binding.
53. Pollak E: Stochastic Transition State Theory. *J Phys Chem Lett* 2018, **9**:6066–6071.
54. Daldrop JO, Kim WK, Netz RR: Transition paths are hot. *EPL Europhys Lett* 2016, **113**:18004.
55. Laleman M, Carlon E, Orland H: Transition path time distributions. *J Chem Phys* 2017, **147**:214103.
56. Jung H, Okazaki K, Hummer G: Transition path sampling of rare events by shooting from the top. *J Chem Phys* 2017, **147**:152716.
57. Jacobs WM, Shakhnovich EI: Structure-Based Prediction of Protein-Folding Transition Paths. *Biophys J* 2016, **111**:925–936.
58. Jacobs WM, Shakhnovich EI: Accurate Protein-Folding Transition-Path Statistics from a Simple Free-Energy Landscape. *J Phys Chem B* 2018, **122**:11126–11136.
59. Woodside MT, Lambert J, Beach KSD: Determining Intrachain Diffusion Coefficients for Biopolymer Dynamics from Single-Molecule Force Spectroscopy Measurements. *Biophys J* 2014, **107**:1647–1653.
60. Cossio P, Hummer G, Szabo A: On artifacts in single-molecule force spectroscopy. *Proc Natl Acad Sci USA* 2015, **112**:14248–14253.
61. Neupane K, Woodside MT: Quantifying Instrumental Artifacts in Folding Kinetics Measured by Single-Molecule Force Spectroscopy. *Biophys J* 2016, **111**:283–286.
62. Edwards DT, Faulk JK, LeBlanc M-A, Perkins TT: Force Spectroscopy with 9- $\mu$ s Resolution and Sub-pN Stability by Tailoring AFM Cantilever Geometry. *Biophys J* 2017, **113**:2595–2600.

- 63\*. Yu H, Siewny MGW, Edwards DT, Sanders AW, Perkins TT: Hidden dynamics in the unfolding of individual bacteriorhodopsin proteins. *Science* 2017, **355**:945–950.  
Atomic force microscope measurements with  $\mu$ s-scale time resolution reveal rapid folding dynamics of helical intermediates of bacteriorhodopsin in native lipid bilayers.
64. Szczepaniak M, Iglesias-Bexiga M, Cerminara M, Sadqi M, Medina CS de, Martinez JC, Luque I, Muñoz V: Ultrafast folding kinetics of WW domains reveal how the amino acid sequence determines the speed limit to protein folding. *Proc Natl Acad Sci USA* 2019, **116**: 8137-8142.